WATER TUNNEL STUDIES OF VORTEX FLOW AND VORTEX-FIN INTERACTION ON THE F/A-18 AIRCRAFT

BY

WILLIAM H. WENTZ, JR.

Institute for Aviation Research and Development

The Wichita State University

Wichita, Kansas

This research has been funded by
NASA Ames-Dryden Flight Center
and the
University of Kansas Center for Research, Inc.

Subcontract 7140-85 - Prime Grant NAG 2-371

July 1986

ABSTRACT

Water tunnel tests have been conducted to study the flow associated with fin buffet for twin-fin fighter aircraft using 1/48th scale F/A-18 models. Flow visualization made use of colored dyes to determine vortex patterns, and surface hot film anemometry was used to study the turbulent energy and the frequencies present in the flow. Configurations tested included the full airplane, airplane without fins, airplane without leading-edge-extensions, (LEX's) and airplane without wings. Test Reynolds number ranged from 4,300 to 12,800, with corresponding Mach numbers less than 10^{-6}.

The flow studies show that the LEX vortices burst just forward of the fins at about 25^{o} angle of attack. Removing the fins had negligible effect on vortex locations and bursting, but removing the wing had a marked effect on both location and burst angle of attack for the vortices. Studies of body vortices with the LEX's removed demonstrated that the body vortices were not a dominant feature of the flow associated with fin buffet.

Hot film anemometer signals show that fin surface turbulence increases with angle of attack, and that dominant frequencies appear in the flow when bursting occurs. The dominant frequencies correspond to a Strouhal number of 0.7 for all speeds tested, and for all angles of attack for which vortex bursting was present. Flow patterns, vortex bursting angles of attack, and Strouhal numbers of the

unsteady flow correlate well with wind tunnel tests from other investigations at higher Reynolds number, confirming the validity of water tunnel testing.

SYMBOLS

c	wing mean aerodynamic chord, (0.24 ft, 1/48th model scale)
f	frequency, Hz
M	Mach number, V/(speed of sound), non-dimensional
Psd	power spectral density of hot film signal, $(\text{Volts})^2/\text{Hz}$
Re	Reynolds number, cV/ν , non-dimensional
S	Strouhal number, fc/V, non-dimensional
V	tunnel velocity, ft/sec
α	angle of attack, degrees
ν	kinematic viscosity, ft^2/sec

INTRODUCTION

Twin-fin arrangements have recently emerged as a configration favored by aircraft designers. This configuration is especially attractive for carrier-based aircraft, since it offers reduced fin height, making hanger access and maintenance easier. The F/A-18 aircraft uses this arrangement, but unfortunately the aircraft has developed fin fatigue problems requiring structural modification. Flight and wind tunnel tests revealed that the un-anticipated fin loads occur at subsonic high angle of attack conditions. These loads are apparently related to the interaction of

vortices emanating from the wing leading edge extensions (LEX's) with the fins.

This report documents tests using small scale models in a water tunnel to visualize the flow phenomena associated with high angle of attack conditions for the twin-fin fighter type aircraft. The primary purpose of this research was to identify the flow associated with fin buffet for this aircraft and to generalize so far as possible from these results, in order to avoid such buffet problems for future designs. A second purpose was to evaluate the water tunnel as a research tool as compared to the more traditional wind tunnel and flight test environments for experimental tests.

EXPERIMENTAL FACILITY

The facility for the experiments reported here was the NASA Ames-Dryden water tunnel flow visualization facility located at Edwards Air Force Base, California. This tunnel is a closed return vertical flow water tunnel, with 16" x 24" test section. Earlier tests of the F/A-18 in a similar water tunnel were reported in reference 1. The tunnel was designed primarily for use as a visualization facility, but in the present tests special surface hot-film anemometry instrumentation was utilized to make quantitative measurements of the unsteady, buffeting flow.

LIMITATIONS OF SMALL-SCALE AERODYNAMIC TESTING

Classical design of fluid dynamic experiments requires "dynamic similarity" of the model and full-scale airplane.

Dynamic similarity is achieved when Reynolds number and Mach number of the model and full-scale airplane are the same, and when the model and full-scale are geometrically similar. In practice, geometric similarity is nearly always achieved by using properly proportioned models. Experiments and theory have shown that matching Mach number is necessary only when compressibility effects become important. This is typically at Mach number above 0.6, depending on thickness ratio. For higher Mach numbers, the pressure distributions are directly affected by compressibility, and Mach matching is essential.

For measurement of skin friction, and precise matching of separation and stalling of airfoils, matching Reynolds number is required. While Reynolds number matching is required in principle, in practice small-scale testing is frequently used, even though it almost always results in Reynolds number below full-scale values. Full-scale, pressurized and cryogenic wind tunnels are facilities in which full-scale Reynolds number is ordinarily achieved. Testing in these facilities is very expensive because of model and operational costs. Fortunately, it is the nature of viscous flow that aerodynamic characteristics are relatively insensitive to Reynolds number. Often Reynolds number differences of factors of 3 or even 10 have relatively small effect on all aerodynamic coefficients except parasite drag and maximum lift coefficients. For the particular case of fighter-type aircraft, which are characterized by thin, highly swept surfaces, operation at low

speed invariably implies high angles of attack, and high angle of attack leads to separation along the leading edges. For such cases, the separation locations are fixed by geometry, and aerodynamic force coefficients and pressure coefficients are essentially independent of Reynolds number. This is borne out by the research of reference 2. It is this peculiar combination of sharp leading edges and high angles of attack that lends validity to small-scale smoke tunnel and water tunnel tests of aircraft designed for supersonic flight. Test planning and interpretation of results must recognize the limitations and the regimes for which testing at Reynolds number substantially lower than full scale may yield useful information.

MODELS

Models were variations of the F/A-18 aircraft, fabricated from 1/48 scale hobby shop kits. The hobby kits are dimensionally sufficiently accurate for tests of this type, so the only modifications required were the addition small-bore tubing to accommodate the dye used for stream tracing, and a mounting strut. Dye tubes were connected to manifolds within the models, which were fed from a separate external dye reservoir for each of the colors desired. In addition, the models were equipped for engine inlet simulation by use of hollow nacelle passages and flexible plastic water siphon tubes attached to the engine exhaust nozzles. By drawing water into the inlets through the siphon tubes at an appropriate rate, it is possible to control the engine mass flow

capture area ratio. This permits proper simulation of streamline patterns around the aircraft. This is particularly important for those regions of flow near the engine inlets, such as the wing leading edges.

Since one purpose of these tests was to evaluate the effects of the various aircraft components on fin buffet, models were designed with several geometric variables. It was less expensive to construct a family of four models with the various configurations than to construct removable hardware for a single model. Wings leading flaps were deflected 34 degrees down, and trailing edge flaps were undeflected for all tests. These settings are consistent with flight at angles of attack 25 degrees and greater. The geometric variables tested are described below.

F/A-18 BASIC MODEL - Complete airplane with leading edge flaps deflected 34 degrees, trailing edge flaps neutral, all tail surfaces neutral.

F/A-18 WITHOUT WINGS - Same as basic model, except wings removed outboard of leading edge extensions (LEX's). This model was used to evaluate the interference effects of the wing and flow fields.

F/A-18 WITHOUT FINS - This model was used to evaluate the possibility that the fin "blockage" might generate an adverse pressure field of sufficient strength to cause premature bursting of the leading edge vortices.

F/A-18 WITHOUT LEX'S - The purpose of this model was to identify the role and interaction of forebody and LEX vor-

tices, and to ascertain possible wing or forebody vortex interactions on the fin.

TEST CONDITIONS

For all tests, inlet flow was established to provide for an inlet capture area ratio of unity. Speed control in the water tunnel is by means of a valve with a series of fixed settings, preventing infinitely variable speed control. Table 1 gives the speeds used for these tests, and corresponding chord Reynolds numbers and Mach numbers.

Table 1 - Test Conditions

Speed (ft/sec)	Reynolds Number	Mach Number
0.25	4,300	0.5×10^{-6}
0.58	9,900	1.3×10^{-6}
0.75	12,800	1.6×10^{-6}

Angle of attack was varied from 0 to 40 degrees, in increments of 5 degrees. At 40 degrees, the model was nearly in contact with the upper wall, so higher angles could not have been tested without the use of an offset sting mount. Video and still pictures were obtained from top and side views in separate runs.

INSTRUMENTATION

Instrumentation consisted of video cassette recording equipment and conventional camera for still photos. In addition, the fin of the basic model was fitted with a strain-gage at the fin root, and two different types of surface hot film anemometers (Disa and Micro-Measurements). These instruments were intended to detect flow unsteadiness over the fin, for correlation with dynamic strain gage data from flight tests.

The Disa hot-film anemometer and the strain gage provided very low-level signals, and these could not be distinguished from random background noise. Only the Micro-Measurements hot film gage provided a signal which displayed characteristics which changed in a consistent manner with angle of attack. Therefore, only the data from the Micro-Measurements hot-film gage was utilized for dynamic measurements. This gage was located at 63% span and 50% chord on the inboard surface of the starboard fin. The output signal from this sensor was monitored on an oscilloscope, and selected signals were also processed using a modal analyzer. The oscilloscope provided real time characteristics of the signal, and the modal analyzer provided frequency analysis of the data in the form of power spectral density (Psd) graphs of the gage voltage. It should be noted that the hot film gage utilized in this manner provides a measure of the heat transfer at the surface. This signal provides a qualitative but not quantitative measure of surface skin friction. The merit in this instrument is the ability to

extract information about the frequencies present in the unsteady flow. Futhermore, these signals can be processed to obtain qualitative differences in turbulent energy levels for the various angles of attack and tunnel speeds.

RESULTS OF FLOW VISUALIZATION

BASIC F/A-18 - The flow video and still pictures show a consistent and repeatable pattern for the vortex flow of this aircraft configuration. Vortex "bursting" or "breakdown" is characterized by an abrupt increase in vortex core diameter, often preceded by a spiralling of the core before complete turbulence ensues. All vortex burst patterns exhibit some unsteadiness, with burst locations oscillating somewhat with time. For this reason, the video images were used as the primary source to determine "average" burst locations. Geometry and vortex burst locations are shown in figure 1. As angle of attack is increased from 0^{o}, vortices form along the LEX's. These vortices increase in strength with angle of attack, and flow aft above the horizontal tail surfaces but beneath the fins for angles below 20^{o}. At 20^{o}, vortex bursting occurs aft of the wing trailing edge and outboard and beneath the fin. At 25^{o} angle of attack, the LEX vortex burst point is located more forward and inboard, with the axis of rotation nearly in line with the fin leading edge. The burst point is slightly forward from the fin leading-edge at this angle of attack. It is difficult to conceive of a vortex burst location which could be potentially more detrimental in terms of introducing fatigue-

producing loads. As angle of attack is increased further, the burst point moves progressively further forward.

F/A-18 WITHOUT FINS - The absence of the fins had negligible effect on the flow field. Vortex locations and burst positions were indistinguishable from the basic model. These results indicate that the pressure gradients associated with the fins are not strong enough to instigate vortex bursting. This is not surprising, considering the small thickness-to-chord ratio of the fins.

F/A-18 WITHOUT WINGS - In this configuration, initial formation of the LEX vortices was in much the same manner as for the full model. As angle of attack was increased, however, the vortices were located more inboard than on the basic model, and they remained intact, without bursting, up to 30° angle of attack. This test series shows important changes in vortex locations and a substantial delay in vortex bursting when the wing is removed. When the wing is present, the adverse pressure gradient field over the aft portion of the wing is evidently a dominant factor in producing vortex bursting.

F/A-18 WITHOUT LEX'S - At high angles of attack, the fuselage forebody, like the LEX's, produces a pair of vortices. This test series shows that the fuselage vortices initially form inboard of the fins, and that they remain inboard of the fins over the entire angle of attack range for which they are visible. At 15° these vortices trail between the fins without bursting. At 20°, bursting occurs

slightly aft of the wing trailing edge, and at 25° the burst location is near wing mid-chord. Burst location remains essentially unchanged as alpha is increased from 25° to 40°. Even at 40°, the spiraling wake of the burst vortices remains close to the fuselage centerline, inboard of the fins. This test series shows that the forebody vortices have much smaller interaction with the fins than the LEX vortices. Studies of the video tapes also show that the spiraling of forebody vortices is at a distinctly lower rate than LEX vortices, indicating lower vorticity associated with the forebody vortices, in agreement with theory.

SUMMARY OF FLOW VISUALIZATION TESTS - Results of the flow visualization test series show that the LEX vortices are the dominant flow feature which provides strong interaction with the fins, and that this interaction is maximum in the 25° to 30° angle of attack range. In this angle of attack range, bursting occurs just ahead of the fin leading edge. Bursting is not influenced by the fins, but is strongly influenced by the presence of the wing.

RESULTS OF HOT-FILM SIGNALS (BASIC MODEL ONLY)

Recently, the "modal analyzer" has been developed for interpretation of dynamic test data, particularly from vibration and flutter testing. This device provides high rate analog-to-digital conversion of signals, with digital storage and processing, including fast Fourier transform techniques (FFT) for determining frequency content of a signal. In addition to its application to strain gage and

accelerometer signals, the modal analyzer is well-suited for analysis of hot film anemometry signals from unsteady or turbulent flows. In the case of fin buffet induced by vortex interactions, it was anticipated that the vortex impingement or vortex bursting process might be periodic, or at least have a characteristic frequency signature which could be used for vibration and fatigue analysis.

The modal analyzer was used to obtain power spectral density (Psd) data for each angle of attack from 0^{o} to 40^{o}. Integration of the Psd data over the frequency spectrum yields energy content of the fluctuating voltage across the hot film gage. The Psd integral is, in turn, a measure of the turbulent energy content of the airstream near the gage. Figure 2 is a graph of energy versus angle of attack. While these data show considerable scatter, the figure clearly indicates a trend of increasing energy content with angle of attack.

Figures 3 through 7 show the power spectra for the various angles of attack and speeds. Peaks in the Psd plots indicate frequencies which are characteristic of the flow. Thus a Psd graph which is relatively flat indicates a flow with no identifiable periodicity ("broad-band" turbulence). In contrast, a Psd graph with distinct peaks is indication of characteristic periodicity within the flow. For angles of attack of 0^{o} to 20^{o}, Psd's are very low-level over all frequencies, and without peaks to indicate a dominant frequency. Since all Psd plots from 0^{o} to 20^{o} appear the same,

only the 20° graph is shown (figure 3). For 25°, a distinct peak appears at V = 0.25 ft/sec, but is not visible for V = 0.58 and 0.75 ft/sec. For angles of attack of 30°, 35° and 40°, energy levels are distinctly higher, and dominant frequencies are discernable at all speeds tested.

To correlate model and full scale periodic phenomena or periodic phenomena for the same model at different speeds, a non-dimensional form of frequency is needed. This is provided by the Strouhal number, which is defined as follows:

$$\text{Strouhal number} = (f \times c)/V,$$

where: f = frequency, Hz

c = wing reference chord

V = free stream velocity.

Presumably, Strouhal number, like lift coefficient and other aerodynamic coefficients, will be relatively invariant with speed and scale. To test for consistency of Strouhal number, runs were made with tunnel speeds of approximately two and three times the nominal value. Dominant frequencies selected from the Psd graphs are plotted as frequency versus velocity for each angle of attack from 20° to 40° in figures 3 through 6. These results, taken from two separate test series, show that dominant frequency tends to increase linearly with tunnel velocity, indicating that Strouhal number is indeed constant with velocity. Furthermore, the Strouhal number is essentially a constant value of 0.7 for all angles of attack for which periodic behavior was observed.

CORRELATION WITH OTHER TESTS

The observation that Strouhal number is approximately constant with velocity is a crucial finding from these experiments. These results lend validity to the use of small scale tests, since they show that Strouhal number is independent of Reynolds number, at least for the test range of velocities. Furthermore, wind tunnel tests of a 12% scale basic F/A-18 configuration at Reynolds numbers of 0.4 and 0.8 x 10^6 by McDonnell-Aircraft Company (ref. 3) have shown nearly the same location for LEX vortices, nearly the same angle of attack for vortex bursting, and nearly the same Strouhal number for unsteady fin surface pressures. These correlations are strong evidence that the fundamental flow patterns are independent of Reynolds number, even for the very low Reynolds numbers of the water tunnel tests. Achieving this correlation for the basic model gives credibility to conclusions from water tunnel test results with the non-standard configurations. The merit of water tunnel experiments is the ability to quickly and inexpensively evaluate trends and essential features of flows associated with a wide variety of configurations. More detailed tests in wind tunnels and flight with a narrower range of configurations are still essential to validate final design configurations.

CONCLUSIONS

1. Surface hot-film anemometry shows high turbulent activity on the fins at conditions coincident with vortex bursting observed from flow visualization.
2. LEX vortex bursting occurs directly forward of the fin leading-edge for angles of attack of 25° and higher.
3. The onset of vortex bursting produces flow unsteadiness with a dominant frequency at a Strouhal number of 0.7 for three speeds and for angles of attack from 25° to 40°.
4. LEX vortex bursting is associated with wing separation and stalling. Removing the wing produced substantial changes in vortex positions and delayed vortex bursting.
5. Vortex bursting is unaffected by the fins. Removal of the fins had no appreciable effect on vortex locations or vortex bursting.
6. Vortex frequencies, vortex bursting, and dominant frequencies from the water tunnel tests correlate well with wind tunnel tests at higher Reynolds numbers.

REFERENCES

1. Erickson, G.E.: "Water Tunnel Flow Visualization and Wind Tunnel Data Analysis of the F/A-18," NASA CR-165859, May 1982.

2. Wentz, W. H. and Kohlman, D. L.: "Vortex Breakdown on Slender Sharp-Edged Wings," AIAA Journal of Aircraft, vol.8, no.3, pp. 165-161, March 1971.

3. McDonnell Aircraft Personnel: "F/A-18 Fin Buffet," Project briefings on fin buffet at Naval Air Development Center (NADC), 21 May 1986.

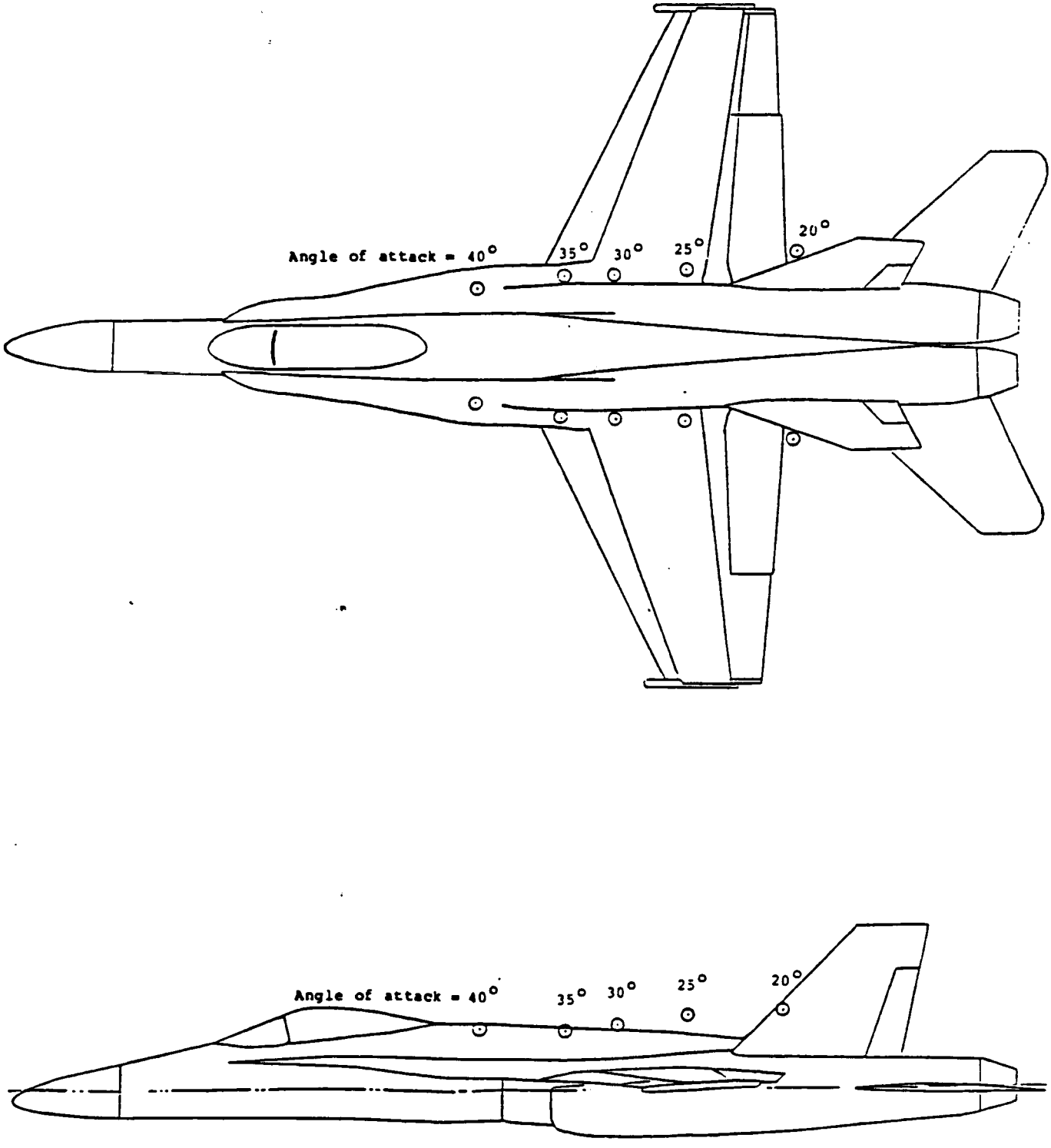

(a) Basic Model

Figure 1. Configurations and Vortex Burst Locations

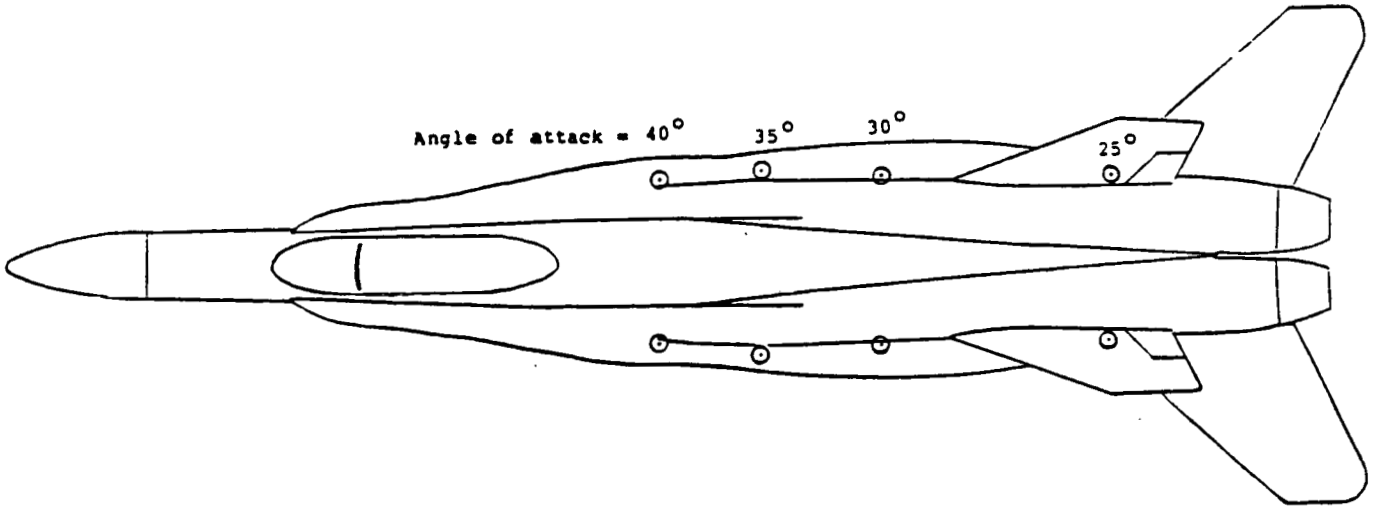

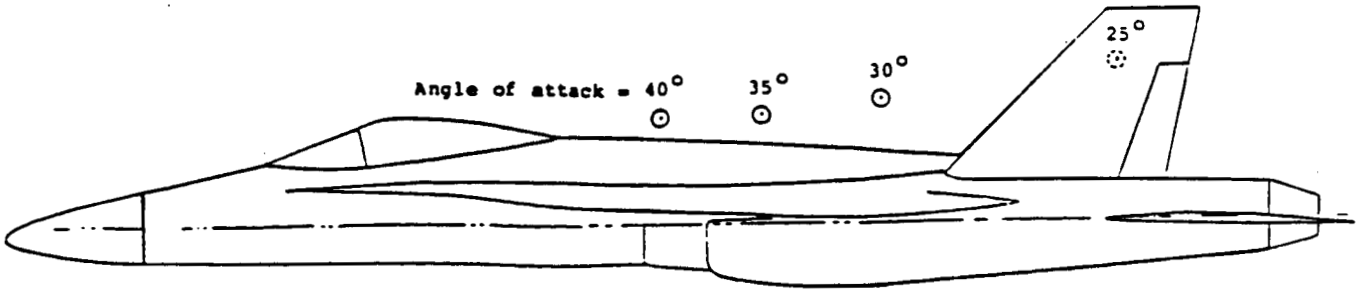

(b) Model Without Wings

Figure 1. Continued.

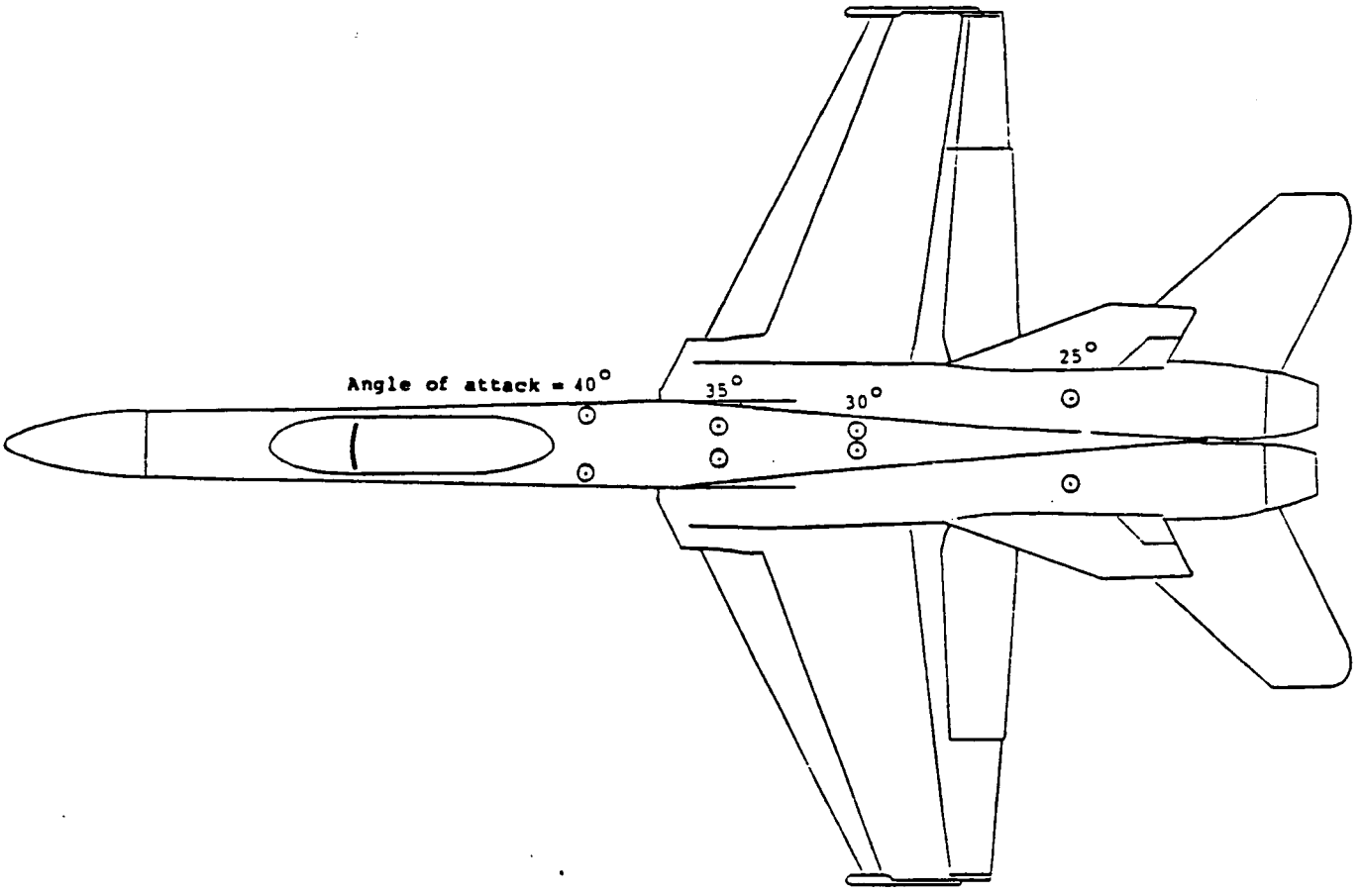

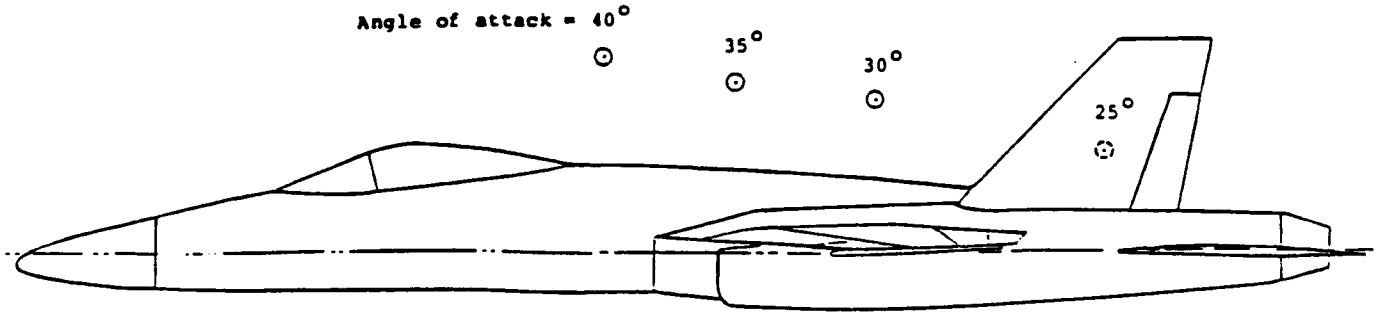

(c) Model Without LEX's

Figure 1. Concluded.

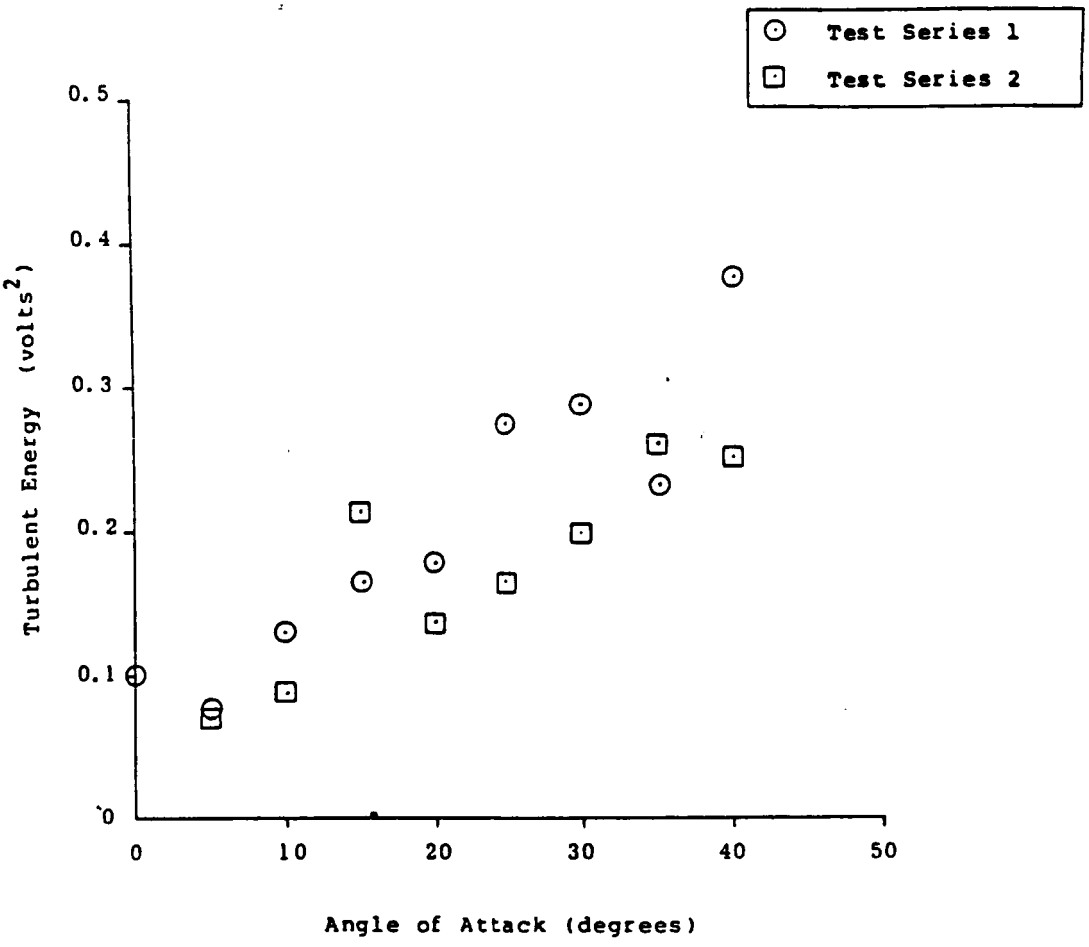

Figure 2. Turbulent Energy at Fin, V = 0.25 ft/sec

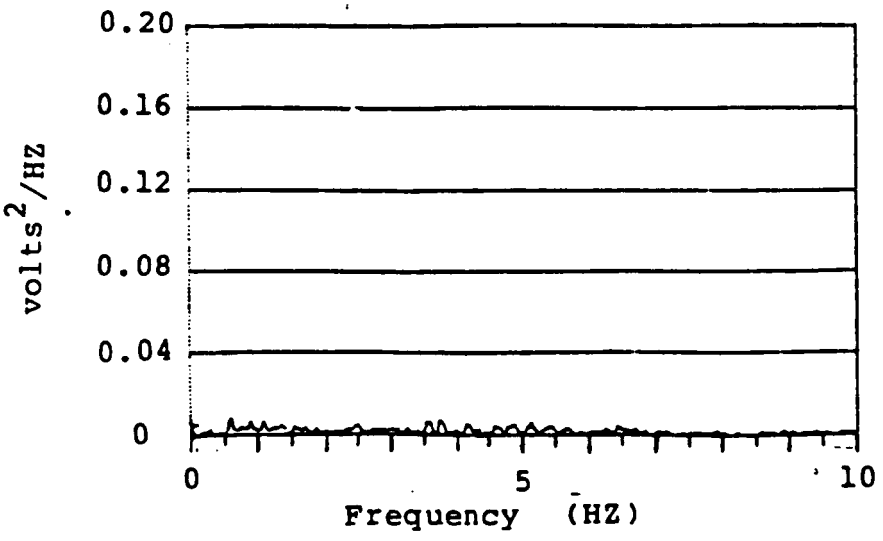

Figure 3. Power Spectral Density, Alpha = 20°, V = 0.25 ft/sec

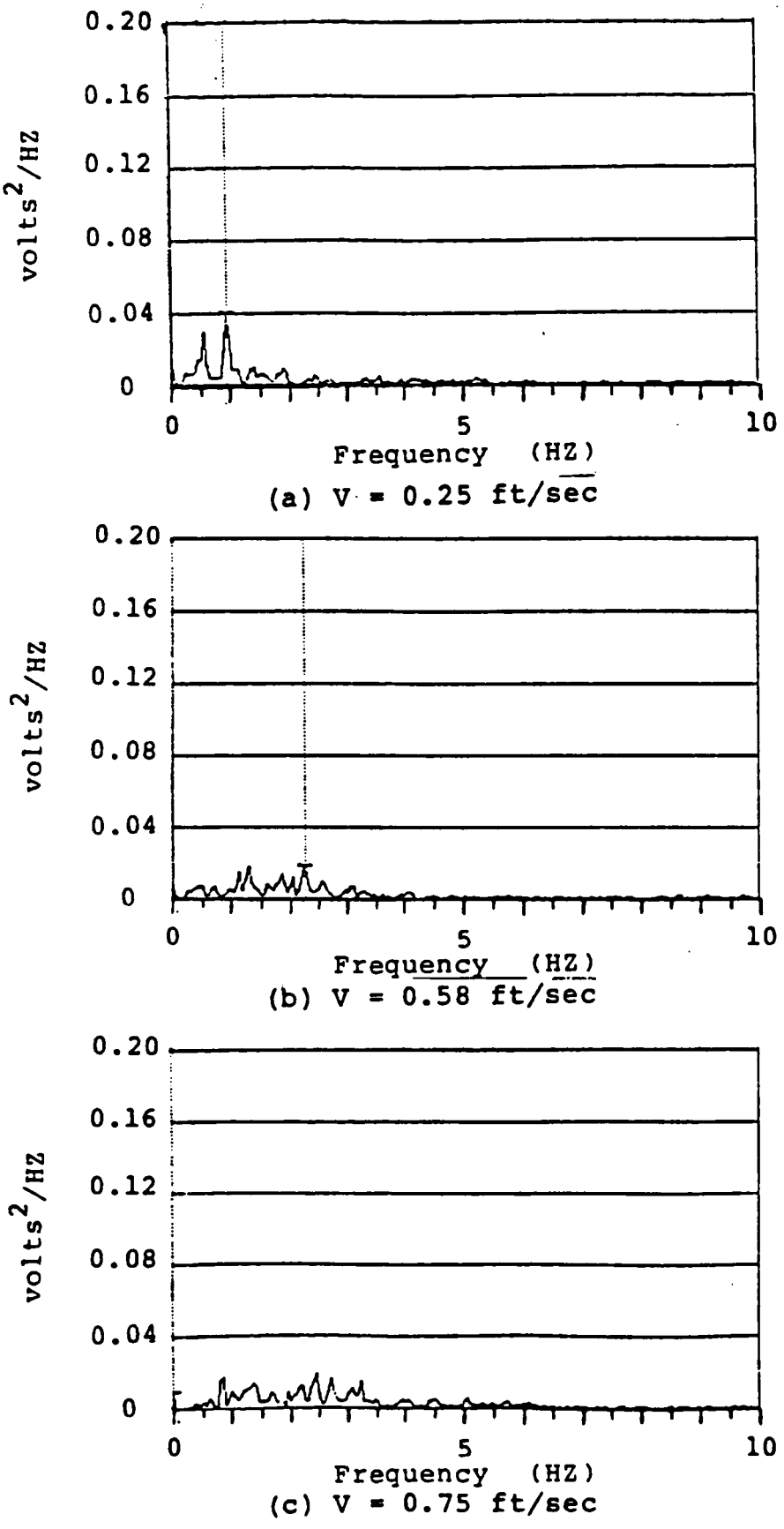

Figure 4. Power Spectral Densities, Alpha = 25°

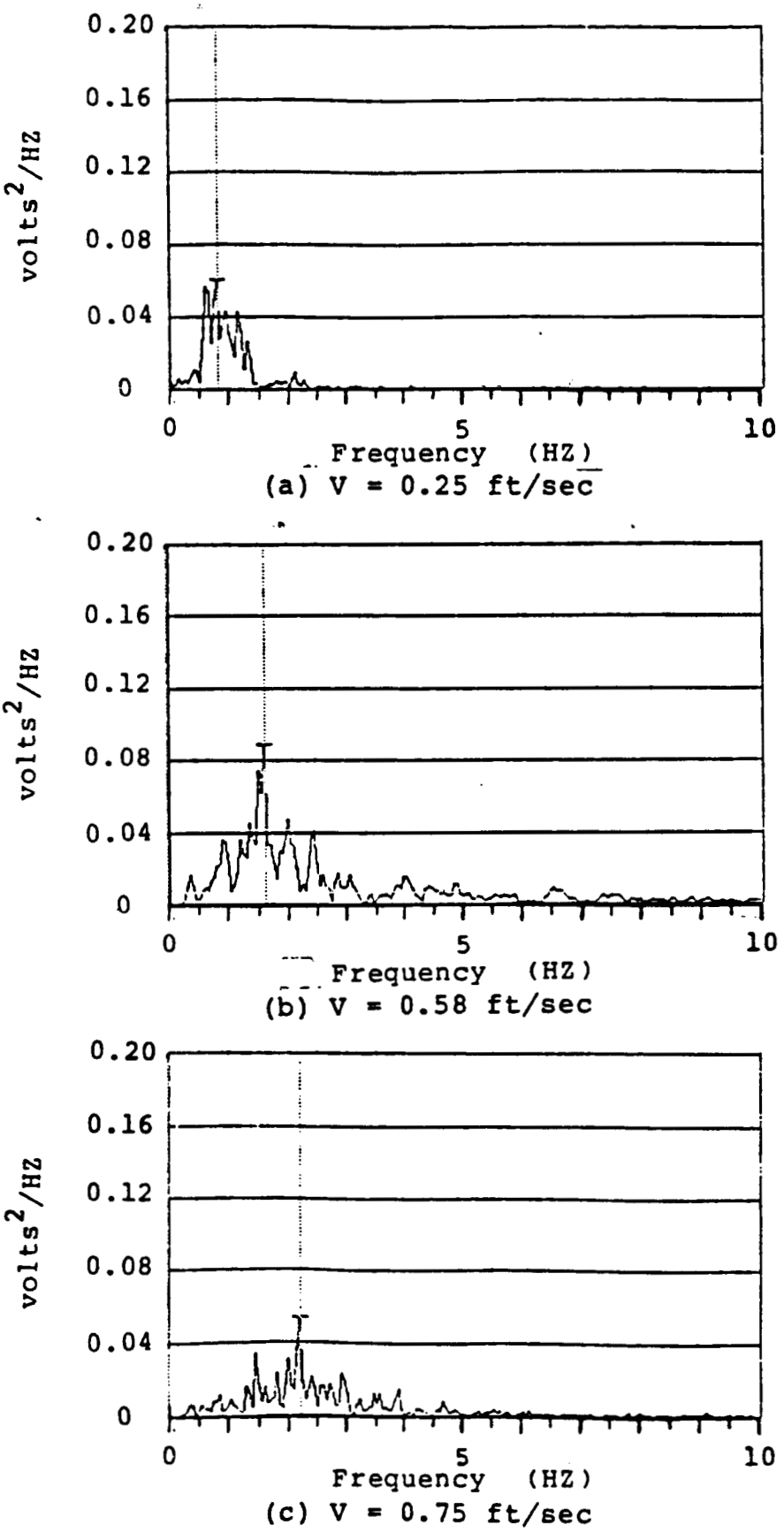

Figure 5. Power Spectral Densities, Alpha = 30°

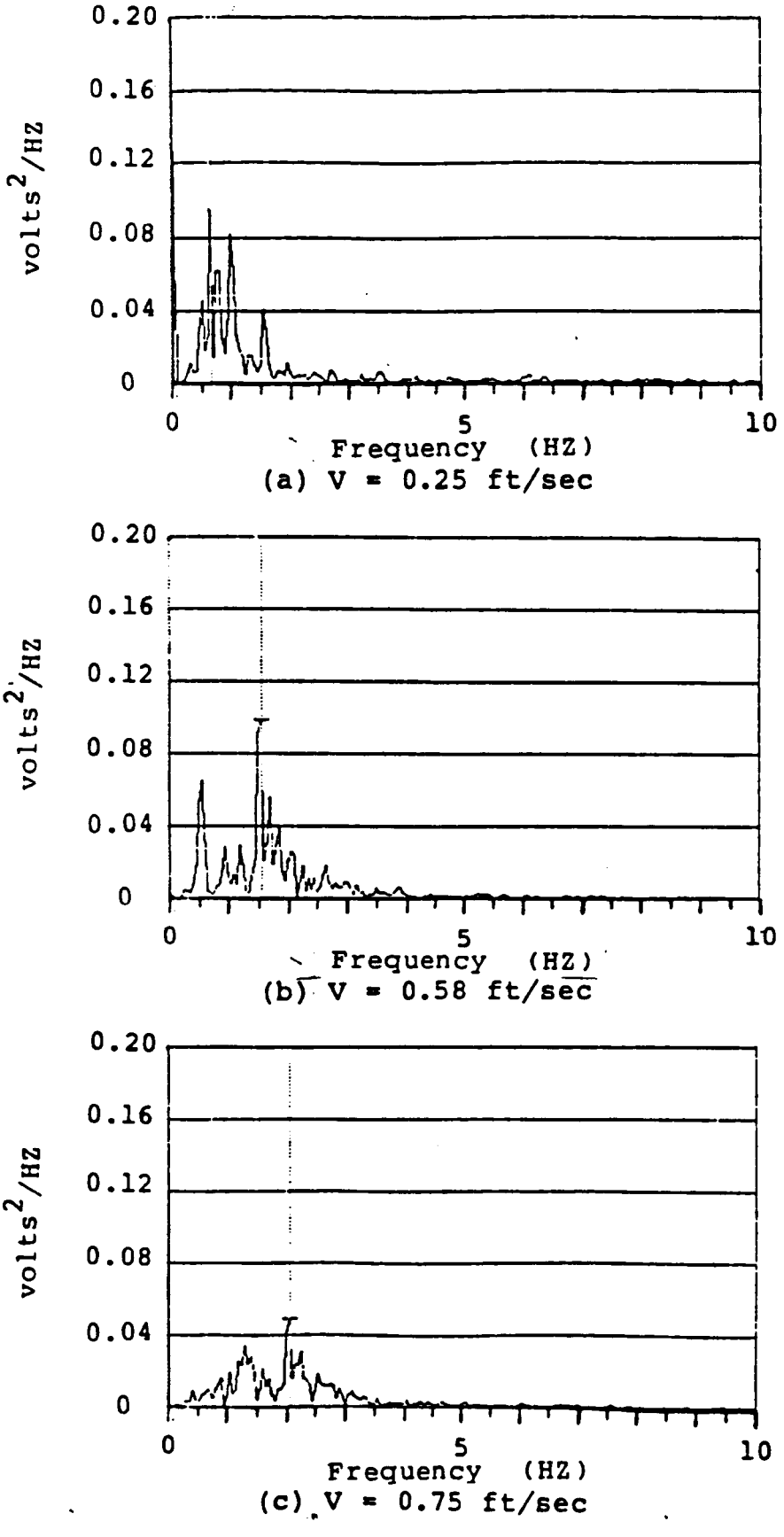

Figure 6. Power Spectral Densities, Alpha = 35°

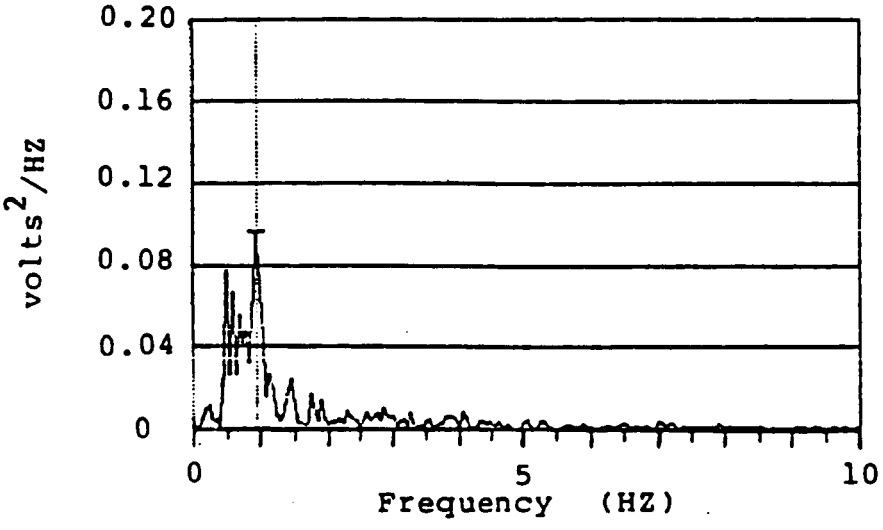

Figure 7. Power Spectral Density, Alpha = 40°, V = 0.25 ft/sec

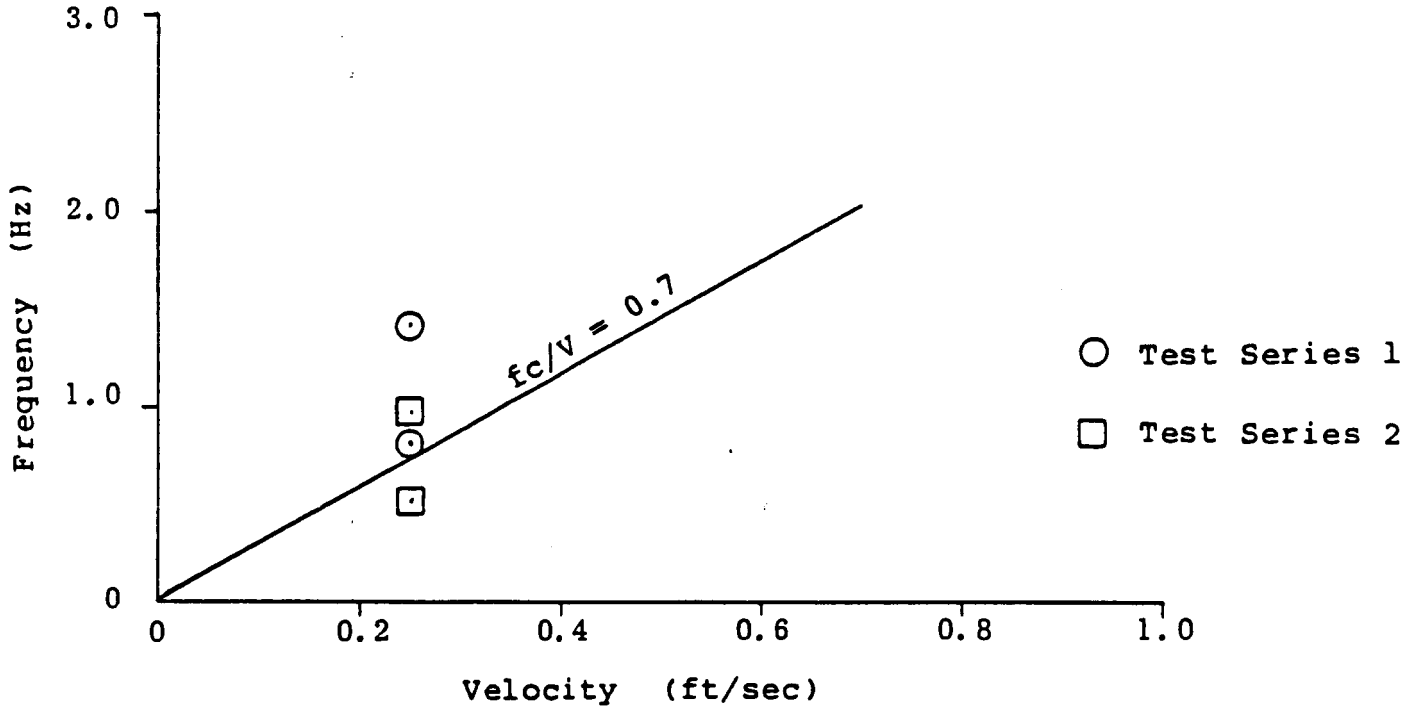

(a) Alpha = 25°

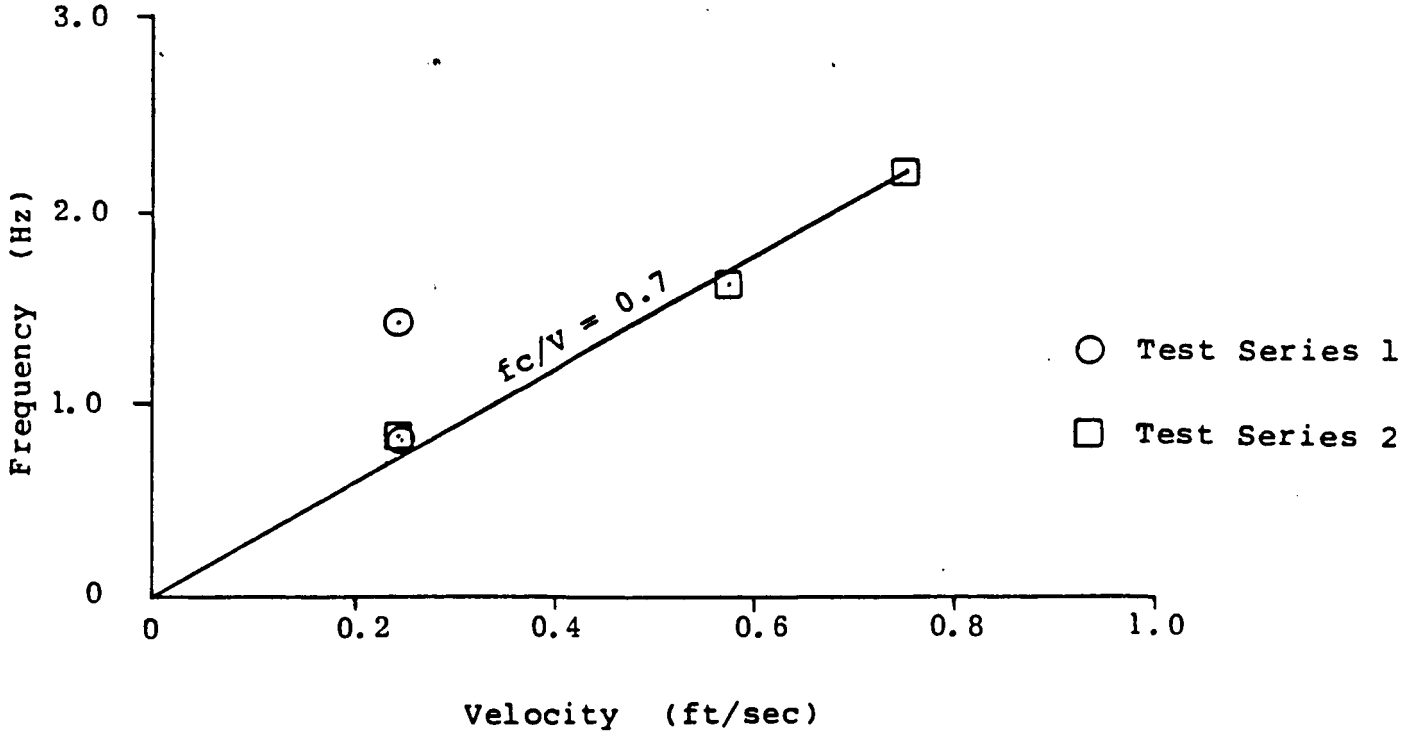

(b) Alpha = 30°

Figure 8. Dominant Frequency and Strouhal Number

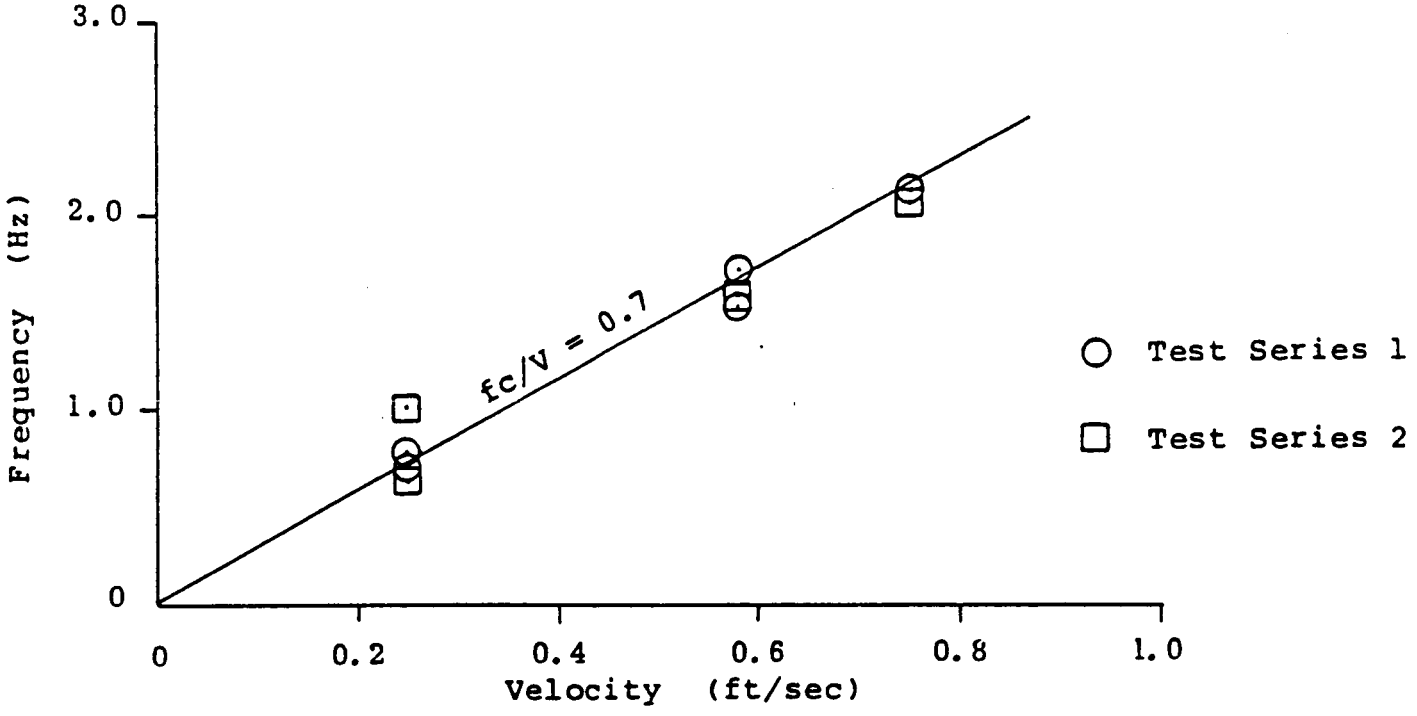

(c) Alpha = 35°

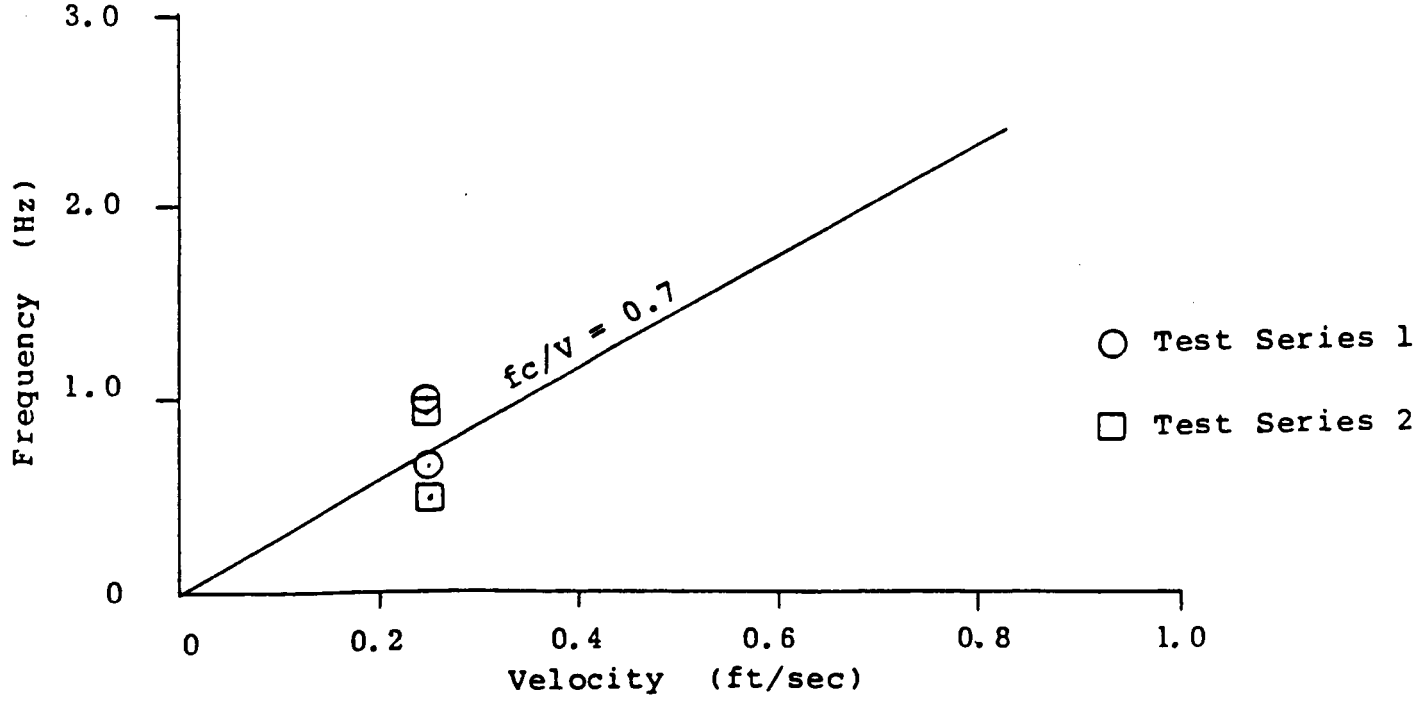

(d) Alpha = 40°

Figure 8. Concluded.

A
20
B
TA
O

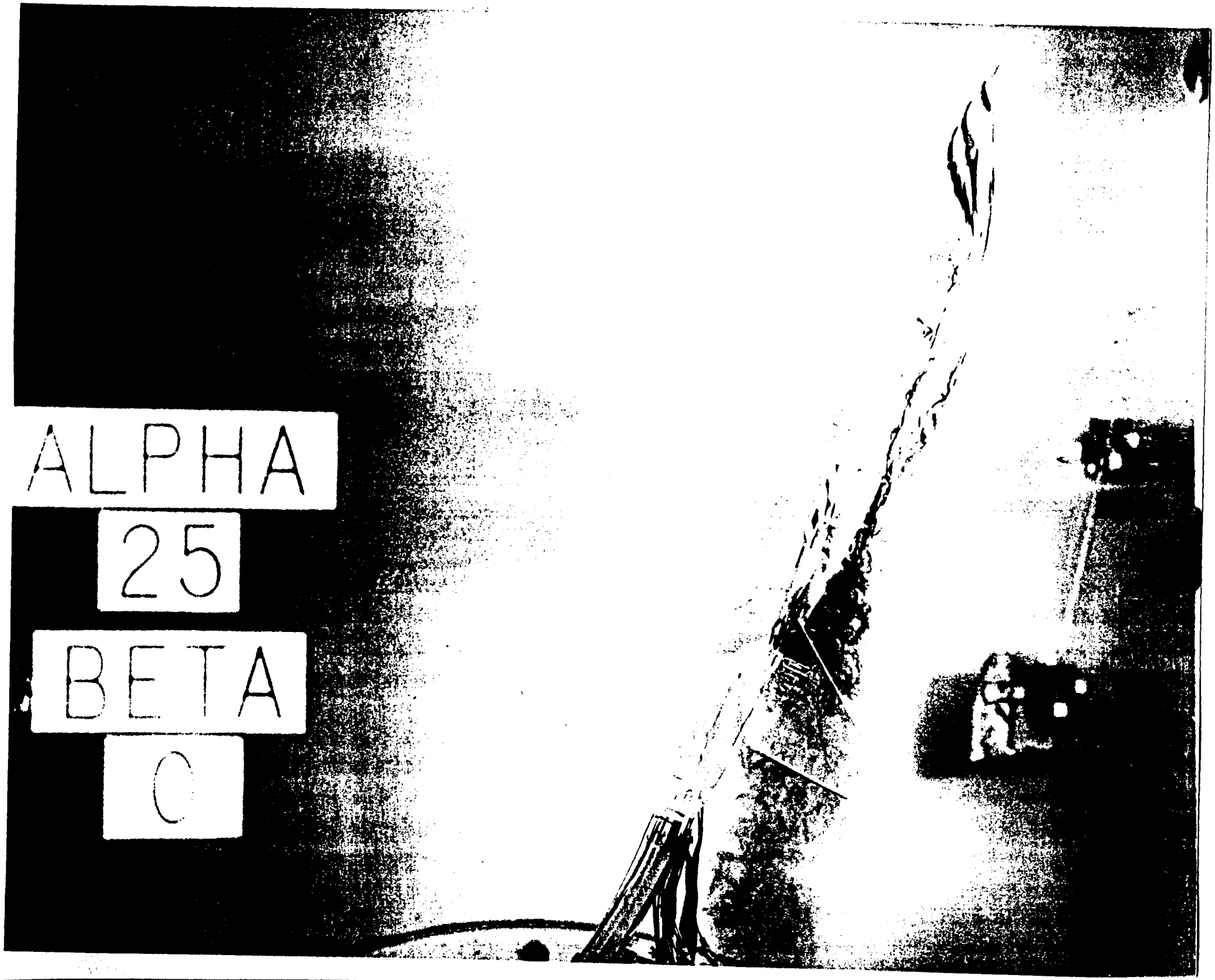
ALPHA
25
BETA
C

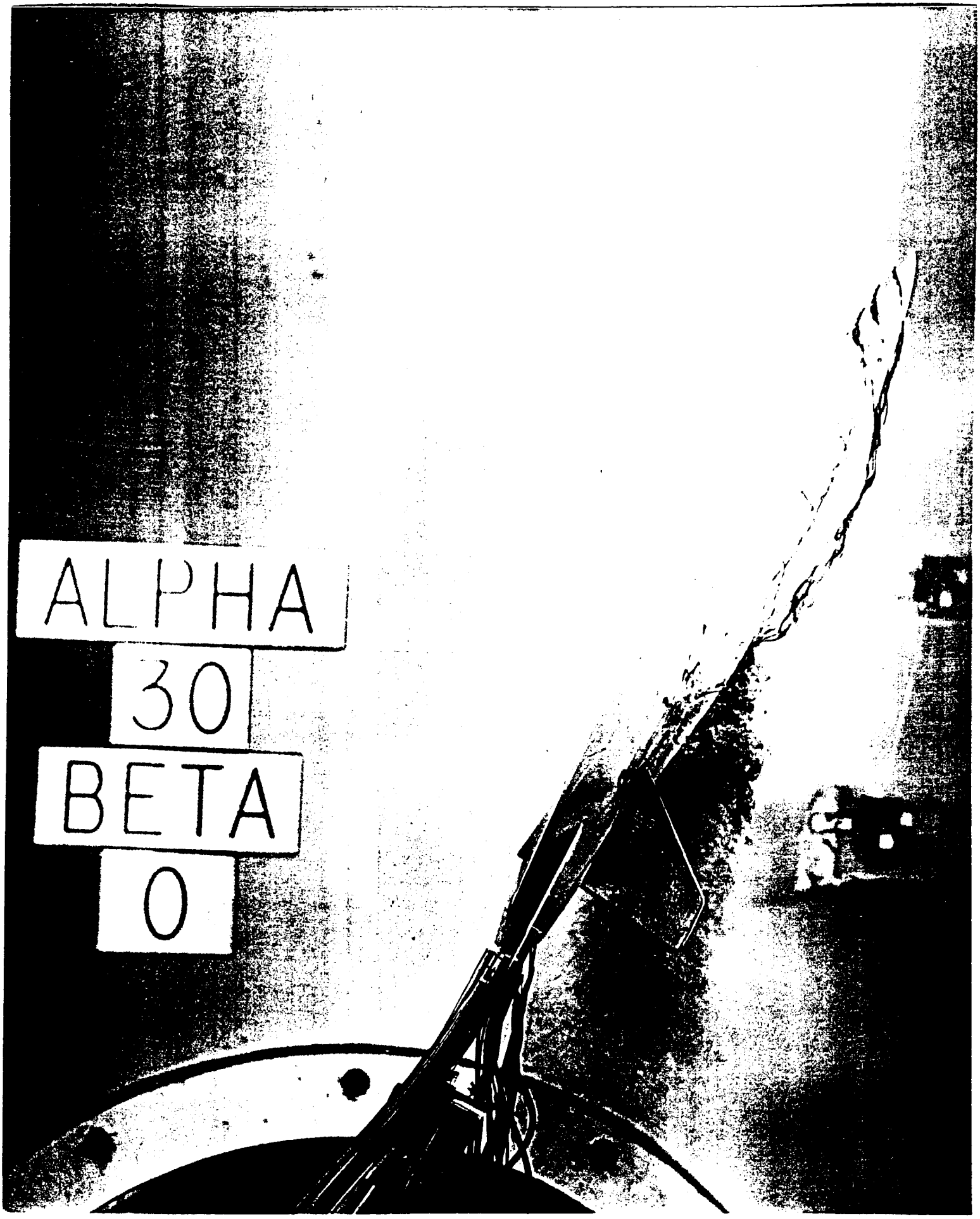
ALPHA
30
BETA
0


ALPHA
35
BETA
0


ALPHA
40
BETA
0


ALPHA
10
BETA
0

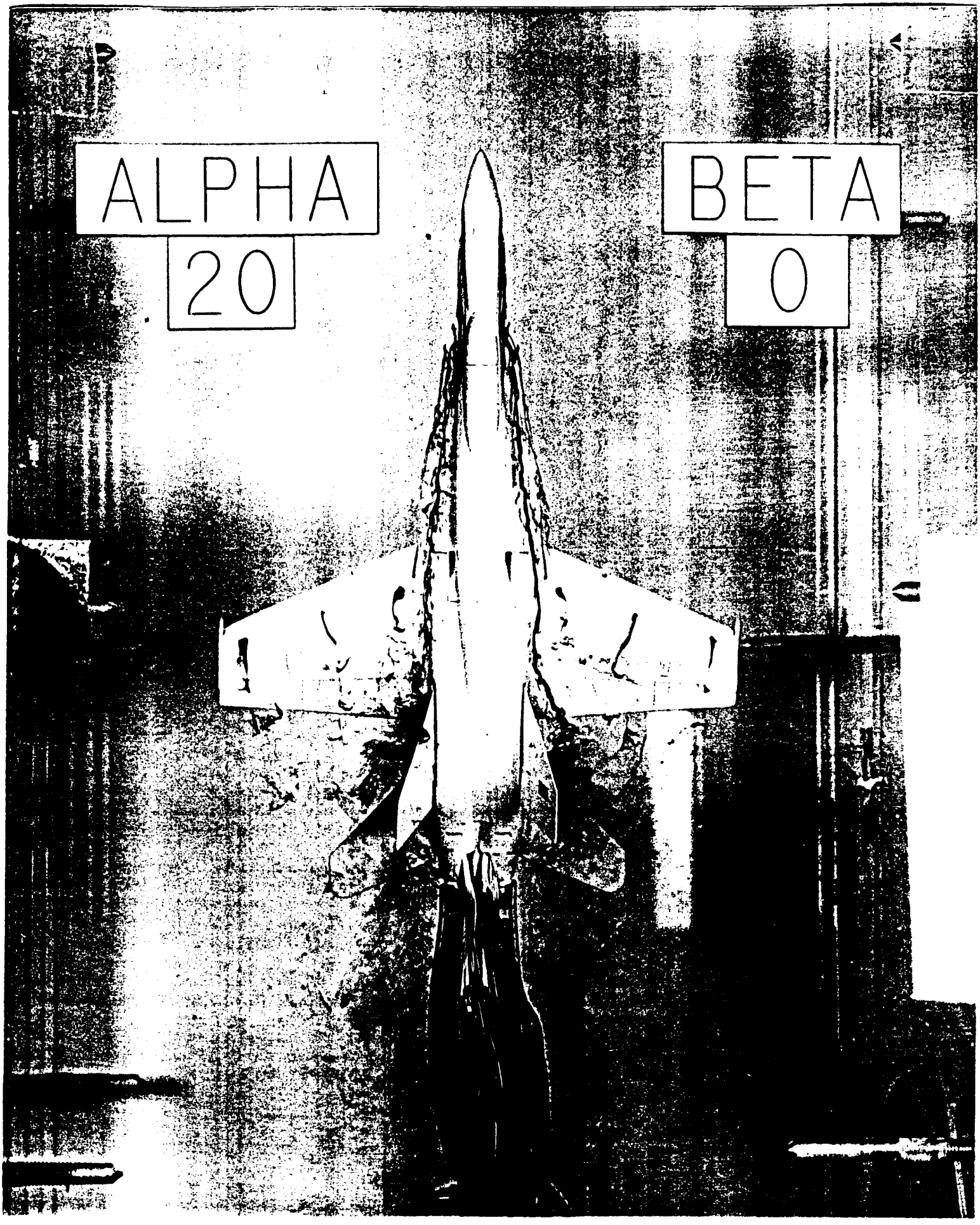
ALPHA
20
BETA
0

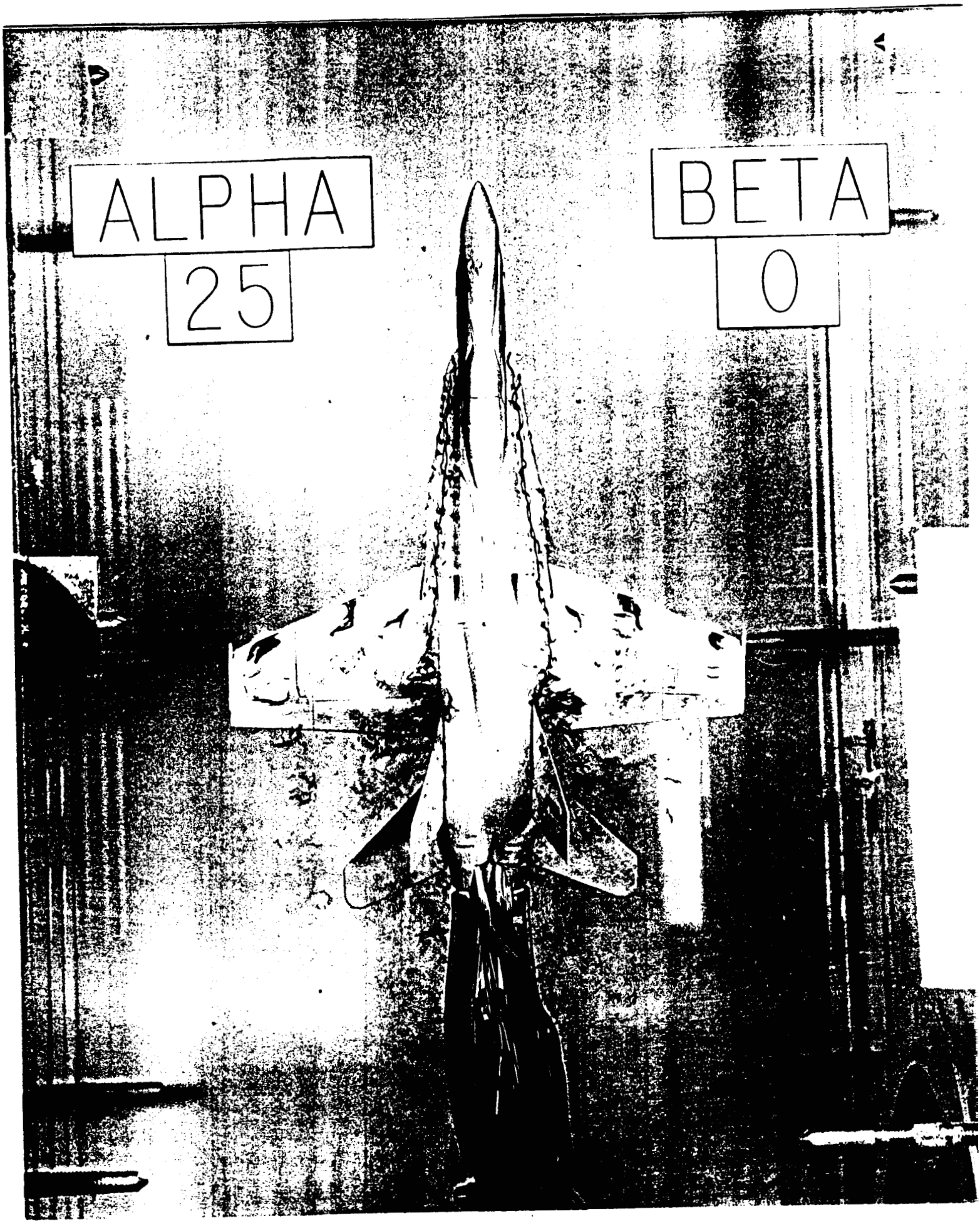
ALPHA
25
BETA
0

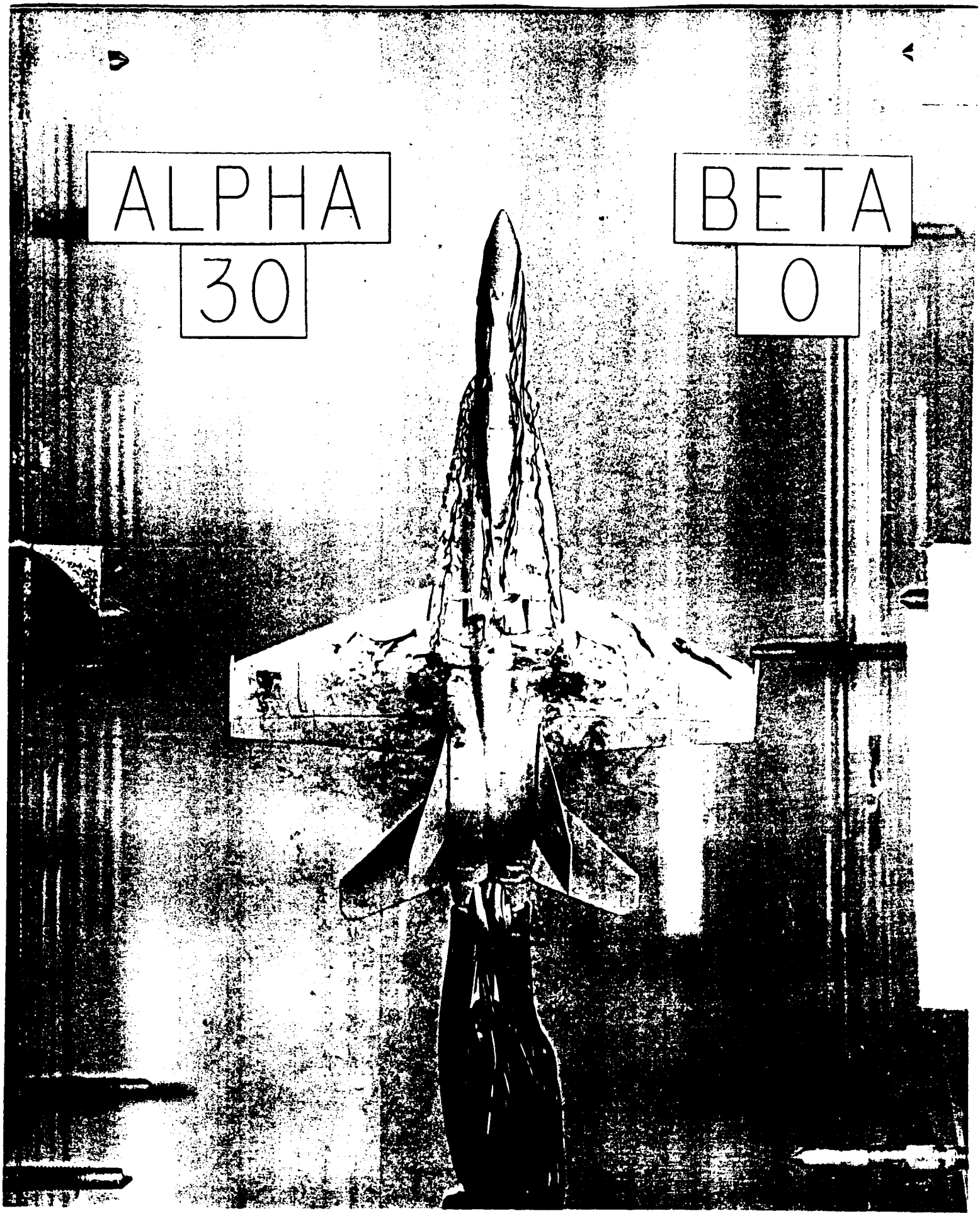
ALPHA
30
BETA
0

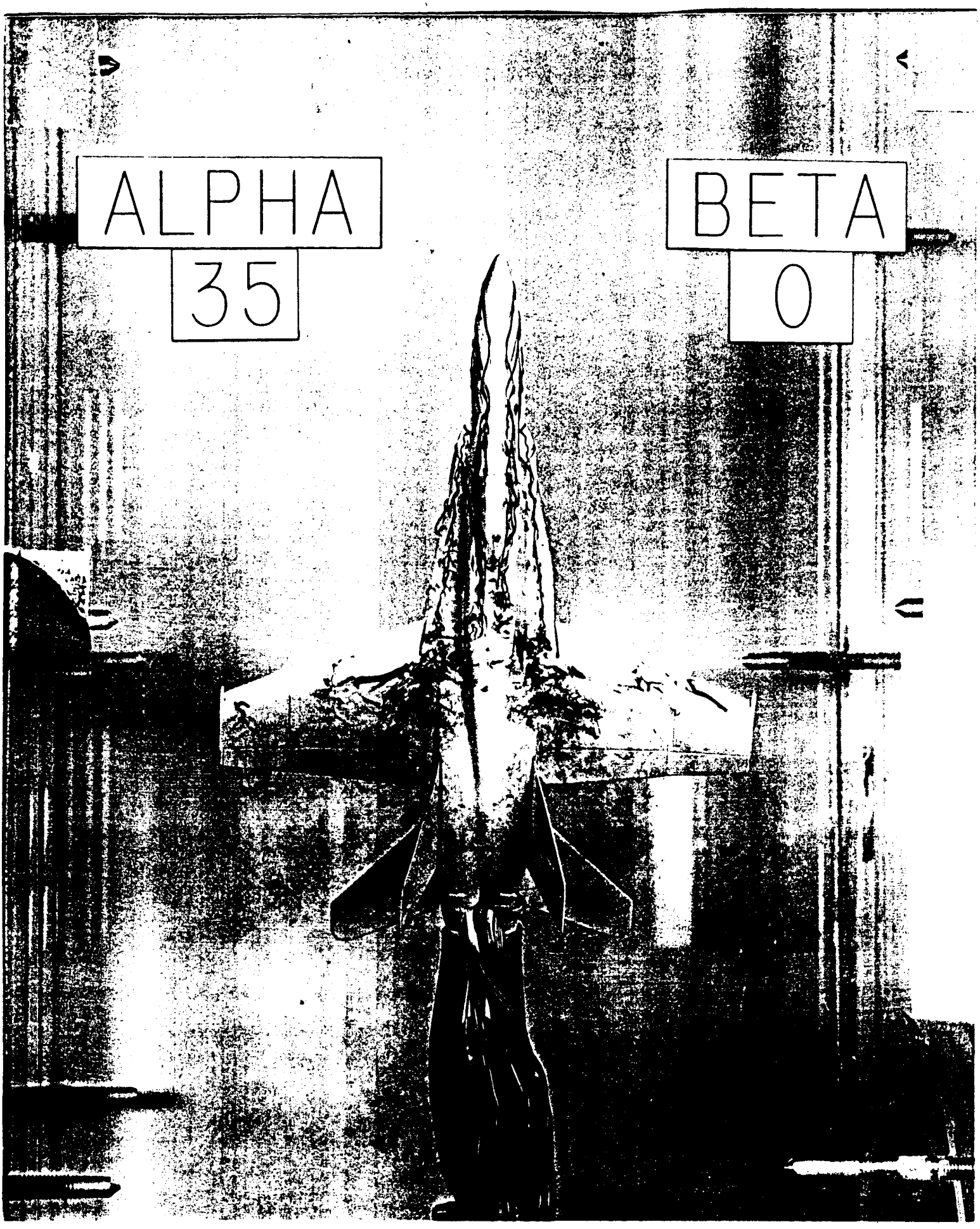
ALPHA
35
BETA
0

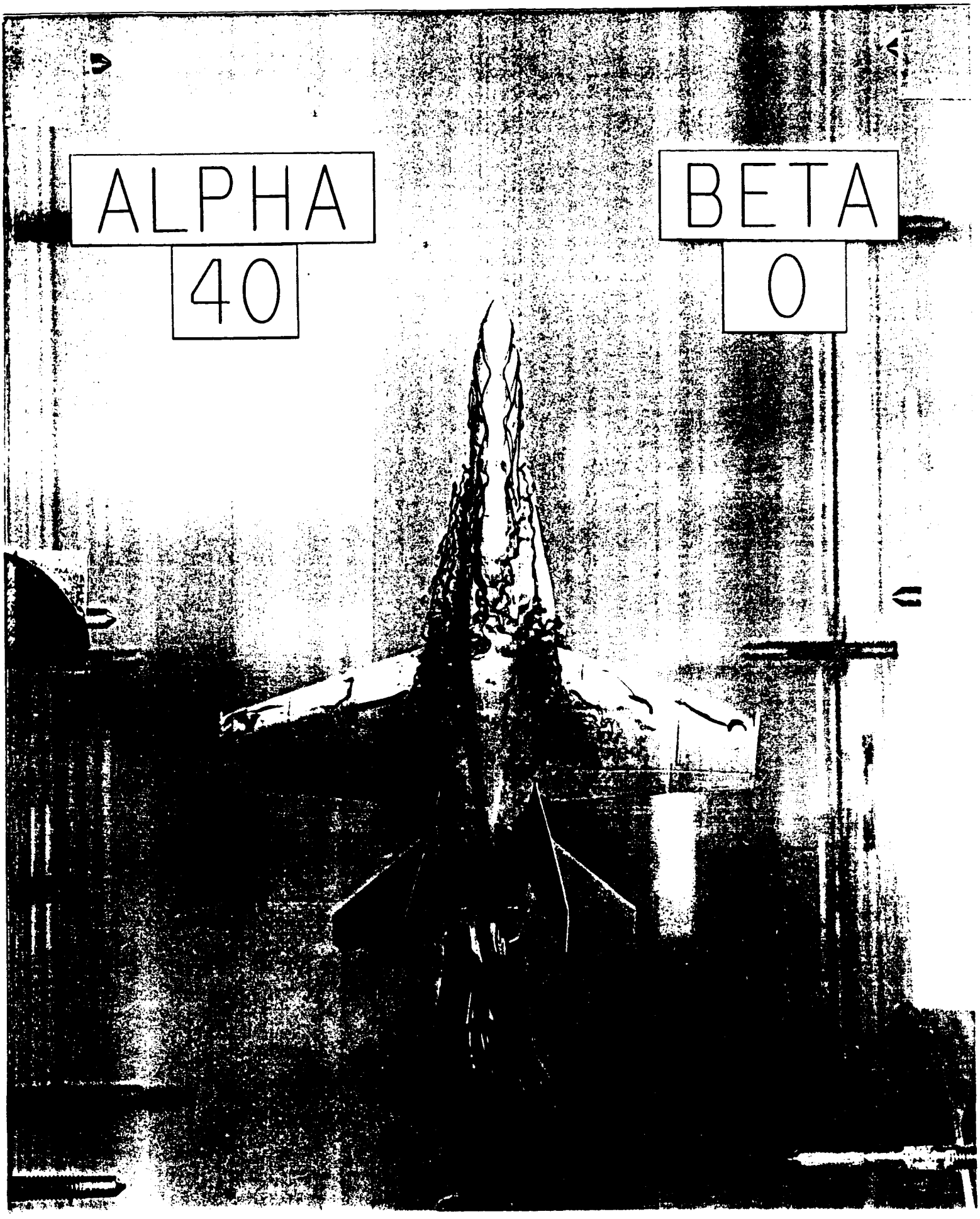
ALPHA
40
BETA
0